NURETH14-253

EVAPORATION OVER SUMP SURFACE IN CONTAINMENT STUDIES: CODE VALIDATION ON TOSQAN TESTS

J. Malet¹, T. Gelain¹, O. Degrees du Lou^{1,2} and V. Daru^{2,3}

¹ Institut de Radioprotection et de Sûreté Nucléaire (IRSN), DSU, SERAC, LEMAC, Saclay, France

² Arts et Métiers ParisTech, DynFluid Lab., Paris, France ³ LIMSI-CNRS, Orsay, France

Abstract

During the course of a severe accident in a Nuclear Power Plant, water can be collected in the sump containment through steam condensation on walls and spray systems activation. The objective of this paper is to present code validation on evaporative sump tests performed on the TOSQAN facility. The ASTEC-CPA code is used as a lumped-parameter code and specific user-defined-functions are developed for the TONUS-CFD code. The tests are air-steam tests, as well as tests with other non-condensable gases (He, CO_2 and SF_6) under steady and transient conditions. The results show a good agreement between codes and experiments, indicating a good behaviour of the sump models in both codes.

Introduction

During the course of a severe accident in a Nuclear Power Plant, water can be collected in the bottom of the containment through steam condensation on walls and spray systems activation. This water can thus be considered as a heat and mass source and/or sink term for the gas mixture composition and thermal state of the containment atmosphere. As a result, heat and mass transfers between sump and atmosphere are generally taken into account in nuclear containment codes. From analysis of real accidental scenarios, it can be deduced that the sump can mainly be in an evaporative state, but boiling and condensing state could also occur. Past studies within the frame of containment calculations have shown that containment codes suffer from a lack of detailed validation of sump modelling. Furthermore, the increasing use of CFD codes shows the necessity of developing a sump model for multi-dimensionnal calculations, whereas it has generally been developed for Lumped-Parameter codes. Concerning IRSN computational tools, the CFD code used for thermal-hydraulic containment studies is TONUS-CFD [1], whereas the lumped-parameter code is ASTEC/CPA [2]. The objective of this paper is to present the calculations of sump tests performed with both codes and to compare them with experiments. The considered experiments are performed in the TOSQAN facility (Tonus Qualification ANalytique). This facility has a lot of specific instrumentation implemented with a high density regarding to its size. It has already been improved for containment code validation such as atmosphere containment mixing by convection and wall condensation [3] or mixing by spray systems [4]. This paper first briefly describes the real sump characteristics known from French nuclear reactor accident scenarios and presents past activities on sump containment codes validation. The TOSQAN sump test matrix is described as well as the code models relative to the sump interaction with the containment atmosphere. At last, the numerical results are compared with the experimental data.

1. State of the art

1.1 French real reactor sump

The sump is located at the basement of the containment vessel, and most of the sump water is generally collected in an annulus surface around the inner vessel. The estimated amount of water in this sump is about 1800 tons, over a surface of approximately 1000 m².

From accidental scenario calculations, it can be considered that either (1) a condensing and/or an evaporative sump with agitated surface (generally due to spray droplets impacting the water surface) at 80°C can be obtained, or (2) an evaporative sump, at around 130°C, in the presence of pressurized non condensable gases (H₂, CO, CO₂, etc.), can occur.

The different accidental sequences show the following states:

- a transient state where the sump is filled-in;
- a recirculation phase, while a kind of thermal equilibrium is reached in the sump;
- a phase where sump boiling occurs after corium flow in the sump or containment vent opening.

The sump pH is generally higher than 9. It is assumed that this cannot modify the steam heat and mass transfers and thus that tests under pure water, for thermal-hydraulics behaviour of the containment atmosphere, are representative of the real sump scenarios.

1.2 Past code validation studies

Past studies drawing conclusions on sump models or sump states have mainly been performed in the frame of general containment thermal-hydraulic calculations. Most of the information collected here concerns OECD International Standard Projects (ISP).

The ISP-23 [5] is based on T31.5 test in the HDR facility (HDR, High Pressure Reactor translated from German). In this test, an overpressure followed by a long-term cooling by natural convection is obtained. It is concluded that the modelling of the condensates (that flow down to the sump), and especially of the condensate distribution and temperature, needs some improvement.

The ISP-29 [6] is based on the HDR/E11.2 test. The latter consists of a sequence of several successive injections (steam, hydrogen, steam) followed by a cooling and a spray phase. It is concluded that the cooling of the condensed water on walls is not well estimated by the codes, leading to a wrong estimation of the water sump temperature.

In ISP-37 [7], the M3 test, in the BMC/Vanam facility (BMC, Battelle Model Containment), focuses mainly on aerosol deposition on walls. The results of this ISP show that the codes overestimate the water sump temperature.

From the different conclusions drawn in those ISPs, it is seen that further code validation on sump modelling is necessary.

2. Description of the experiments

2.1 Experimental facility

Experiments are performed in the TOSQAN facility (Figure 1). It is a closed cylindrical vessel (7 m³ volume, 4.8 m height, 1.5 m internal diameter), having thermostatically controlled walls by heated oil circulation in a double stainless steel shell. The available instrumentation in the TOSQAN main volume concerns injection mass flow-rates (steam and/or non condensable gas), gas temperatures, steam and/or helium/non condensable gas volume fractions measured by mass spectrometry [8] and vessel total pressure. The facility provides also numerous possibilities of optical diagnostics [9] which are not used here for sump tests. The TOSQAN sump is a small vessel of 350 litres, with an internal diameter of 684 mm, connected on the basement of the main vessel. It consists of a double stainless-steel wall in which the heated oil is circulated in connection with the so-called lower wall part of the main vessel. A sampling manifold for mass spectrometry is available above the sump interface, for gas concentration measurements, as well as three dense bundles of 32 thermocouples allowing the recording of two horizontal and one vertical temperature profiles.

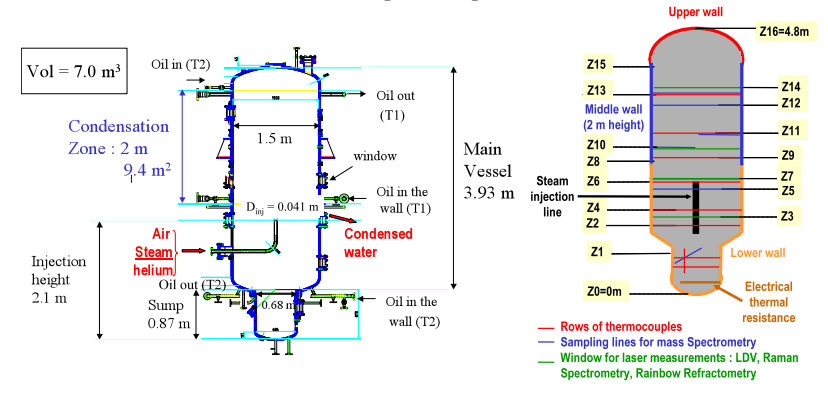


Figure 1: TOSQAN facility and associated instrumentation.

2.2 Test matrix

The TOSQAN sump tests are mainly based on the following test sequence: the vessel is initially closed with dry air at a given thermal equilibrium obtained from the imposed wall temperatures: a so-called 'condensing wall', i.e., the middle wall, of 2 m height, at 2.6 m from the bottom of the vessel, and a so-called 'non-condensing wall', corresponding to the remaining walls, i.e., the upper, the lower and the sump walls (right hand side of Figure 1). At a given time, steam is injected in the vessel, and an equilibrium state is obtained: the total pressure is constant, and the steam injection mass flow-rate is equal to the wall condensation mass flow-rate. Following this equilibrium, steam injection is stopped, vessel depressurization occurs and a second thermal equilibrium state is reached. The water is then injected into the sump, and, after a given time, heated with an electrical thermal resistance: a third steady-state is reached where the sump evaporation and the middle wall condensation mass flow-rates are equal.

The sump reference test (Test 201) is starting at 1.0 bar total pressure and 115° C dry air average temperature. The steam is injected with a mass flow-rate Q_{steam} of 12.5 g/s at the temperature T_{inj} of 127°C, during 2000 s. An equilibrium is reached and the liquid water is then injected at the bottom of the facility with a flow-rate Q_{wat} of 50 g/s at the temperature T_{inj_wat} of 30°C. A power $P_{therm} = 3.22$ kW is used to heat the sump. Wall temperature conditions are around 120°C for the non condensing wall, and around 103°C for the condensing walls. More details are given in [10].

Other tests [11] have been performed on the same basis of this reference test. Tests 202 and 203 are roughly the same kind of tests as Test 201, in which the thermal-hydraulic conditions have been changed in order to reach different levels of evaporation rates. Tests 204 and 205 have been designed with addition of added non-condensable gas. Test 205 is performed with helium (injected at a massflow rate of 0.9 g/s at the same time as liquid water) generally used in thermal-hydraulic containment studies in order to represent hydrogen. In order to enhance the influence of a non-condensing gas on heat and mass transfers over the interface, heavy gases are used in Test 204a (SF₆, injection mass-flow rate about 1.5 g/s) and 204b (CO₂, injection mass-flow rate about 1.5 g/s). Tests 206 and 207 are 201 tests ended with a depressurization performed by opening a valve on the top of the facility, leading to slower or faster depressurization, depending on the valve position.

3. Numerical calculations

3.1 **ASTEC/CPA** [2]

The ASTEC/CPA model includes convection and a possible evaporation or condensation at the water surface, as well as two models depending on the thermal-hydraulic conditions: evaporative or boiling conditions. The heat transfer due to radiation is neglected. The ASTEC/CPA calculations are performed with 5 compartments using the ASTEC/CPA v.13 Rev.3. Associated volumes and surfaces are presented on Figure 2.

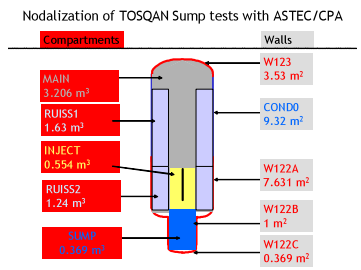


Figure 2: ASTEC/CPA nodalization for TOSQAN sump test calculations.

3.2 Sump model developed for TONUS-CFD [1]

The evaporation sump model presented here is based on a source term modelling using external user-defined functions in a CFD approach. The sump is considered as a surface on which are applied the following boundary conditions: (1) steam evaporation mass flow-rate, (2) a gas-liquid interface temperature. The flow inside water sump volume (convective recirculations) is thus not modelled. These two parameters are both depending of the atmosphere conditions inside the vessel and on the heating power applied to the sump water. They are obtained from mass and energy balance presented in detail in [12]. In this paper, focus is given on the evaporation state and boiling is not considered (the

boiling modelling is presented in [12]). Here, the evaporation mass flow-rate is calculated from two models: one is a purely empirical correlation (so-called "Sump global correlation", described in [13] and in [14]) and the other one is a semi-empirical approach obtained using heat and mass transfer analogy (so-called "Sump HMTA semi-empirical correlation"). The latter is presented in this section and is mainly based on the wall condensation modelling developed for TONUS-CFD [1]. The overall sump model is added to the TONUS-CFD code (v. 2010) using external sub-routines, but can be easily handled in any CFD code allowing external user-defined functions.

3.2.1 Semi-empirical heat and mass transfer analogy (HMTA) model

The evaporation mass-flow-rate Q_{e-emp} is calculated using the following relation:

$$Q_{e_{emp}} = k \rho(T_{bulk}) S_{sump} \frac{\left(Y_s(T_{sat}) - Y_s^{bulk}\right)}{1 - Y_s(T_{sat})}$$
(Eq. 1)

where Y_s is the steam mass fraction, exponent "bulk" stands for the bulk gas mixture, subscript "sat" for the saturation (i.e. for the interface temperature), ρ is the average density, S_{sump} is the sump interface surface, and k is the mass transfer coefficient given by:

$$k = \frac{Sh \ D_m}{L} \tag{Eq. 2}$$

where D_m is the gas mixture diffusion coefficient, and L a characteristic evaporation length. It will be shown that the overall mass flow-rate can be independent of this length.

Applying heat and mass transfer analogy on the sump surface, the Sherwood number Sh can be expressed using turbulent natural convection correlation:

$$Sh = 0.13 \times Ra^{1/3}$$
 (Eq. 3)

where Ra is the Rayleigh number:

$$Ra = Gr Sc$$
 (Eq. 4)

and Sc and Gr are resp. the Schmidt and the Grashof numbers. For evaporation/condensation phenomena, an hybrid Grashof number can be defined on the basis of density differences:

$$Gr = \frac{g \left[\rho_m (T_{sat}) - \rho_m (T_{bulk}) \right] L^3}{\rho_m (T_{bulk}) v_+^2 (T_{bulk})}$$
(Eq. 5)

where g is the gravity and ν_m is the gas mixture kinematic viscosity. The Schmidt number is defined by:

$$Sc = \frac{v_m}{D_m}$$
 (Eq. 6)

Replacing the Grashof number in the mass transfer coefficient expression (eq. 2), using the relation between the kinematic and the dynamic viscosity, and introducing the resulting relation in the mass flow rate equation (eq. 1), the latter is then written:

$$Q_{e_{emp}} = 0.13 \ D_{m}^{2/3} \left(\frac{\rho_{m}(T_{sat}) - \rho_{m}(T_{bulk})}{\rho_{m}(T_{bulk})} \right)^{1/3} \left(\frac{g \ \rho_{m}(T_{bulk})}{\mu_{m}} \right)^{1/3} \rho_{m}(T_{bulk}) S_{sump} \frac{\left(Y_{s}(T_{sat}) - Y_{s}^{bulk} \right)}{1 - Y_{s}(T_{sat})}$$
(Eq. 7)

where it can be seen that the characteristic length L does not appear anymore. This relation is also interesting since it takes into account the densities and the mass fractions in the bulk (i.e. here the values of the variables in the first cell close to the sump interface) as well as at the interface (i.e. here the values of the variables at gas-liquid interface temperature) and does not depend on a global average value on the whole vessel.

3.2.2 <u>Discretization and meshing</u>

In the first part of the TOSQAN sump tests, no water is present in the sump. As a result, calculations are performed on the whole TOSQAN vessel, including gas calculations in the sump (see the so-called 'whole mesh', Figure 3). In the second part of the TOSQAN tests, water is injected into the sump until a given level, and CFD calculations are performed on a so-called 'truncated mesh', where the bottom horizontal line (surface) represents the sump gas-liquid interface (see the bold lines on Figure 3, right part). It has been estimated by mass balance calculations that the sump filling, and the associated piston effect, is negligible on the vessel atmosphere and temperature levels, and thus on the gas distribution. Accordingly, the velocity field should not be changed (velocity values are very low at this stage of the test sequence). Results of the first calculations obtained on the 'whole mesh' are thus projected on the 'truncated mesh' to link up both calculations with or without the sump volume. Sensitivity studies were performed in order to check the influence of several typical modelling parameters such as mesh refinement that did not exhibit major differences.

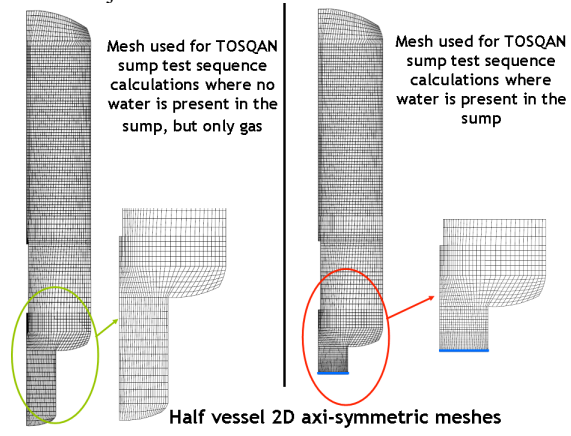


Figure 3: Mesh used for TOSQAN sump test calculations; mesh size around 2 to 4 cm.

4. Results

During this work, results have been obtained with TONUS-CFD and ASTEC/CPA codes for tests 201, 202, 204b, 205. Tests 206 and 207 have only been calculated with ASTEC/CPA. Since test 201 has already been presented in a former paper [12], some figures for this test will not be recalled. For all other tests, a selection of typical results is presented. The typical sump test is presented on Figure 4, where the experimental and numerical results for the total pressure and the condensation mass flow-rate are compared, and on Figure 5 for gas and liquid temperatures. A good agreement is observed on this test, as well as on all other TOSQAN tests, indicating a good behaviour of our sump modelling. A

small difference of pressure is obtained during the evaporation steady-state. Since the condensation mass flow-rate is well reproduced in the code, this difference can be attributed to the mass transfer expression, i.e. either the mass transfer coefficient or the diffusive term generally function of mass fractions in the bulk and at the interface. In the mass transfer coefficients, several other parameters (Sherwood correlations, diffusion coefficient) can also be part of the reason for such differences, that remains, for safety considerations, negligible. A typical vertical temperature profile during evaporative sump steady-state is presented on Figure 6 for both sump models developed for TONUS. It can be seen that the heat and mass transfer analogy modelling (semi-empirical correlation) provides an improvement of the temperature results calculated above the sump interface compared to the sump global empirical correlation. An example of the steam volume fraction and the temperature field is presented on Figure 7 which shows typical gas and temperature distribution patterns for evaporative sump steady-states in all TOSOAN tests. It is also found that the flow is axi-symmetrical, which is confirmed in the experiments, with vertical gas temperature variations (hot air close to the sump interface). During evaporative sump steady-state, the gaseous mixture is, in most of the test, homogeneous, except in the region close to the sump interface where the evaporation leads to mass concentration gradients.

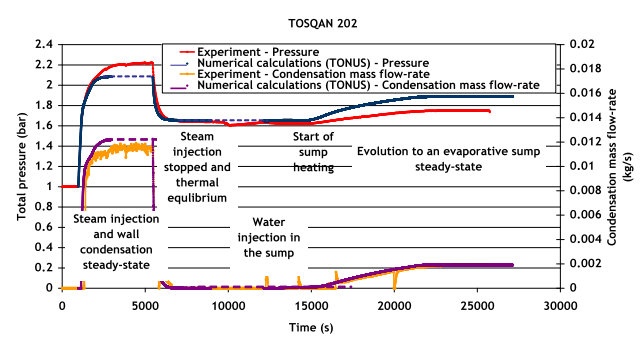


Figure 4: Total pressure and condensation mass flow-rate time evolutions in TOSQAN Test 202, TONUS-CFD results compared to experiment.

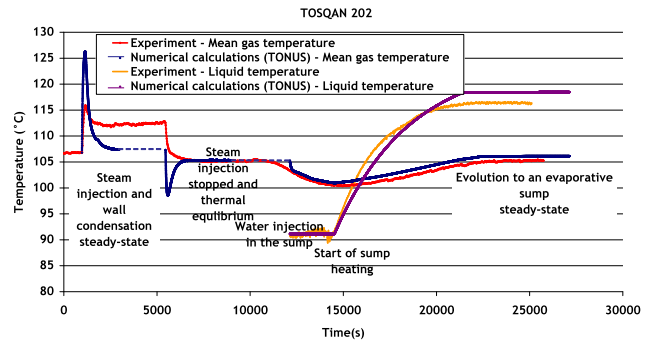


Figure 5: Time evolutions of mean gas temperature and liquid interface temperature – TOSQAN Test 202, TONUS-CFD results compared to experiment.

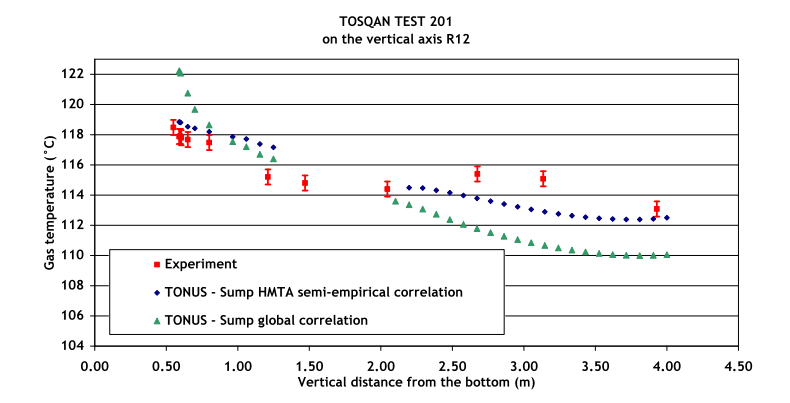


Figure 6: Vertical temperature profile during evaporative sump steady-state, TOSQAN Test 201, TONUS-CFD results compared to experiment for both implemented sump models.

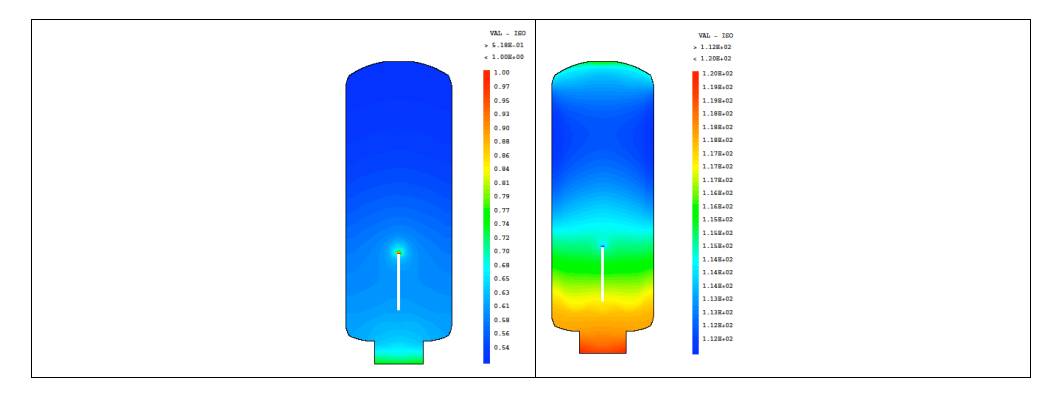


Figure 7: Steam volume fraction (left) and gas temperature (right, in °C) during evaporative sump steady-state, TOSQAN Test 201, TONUS-CFD results.

 ${\it Macintosh~HD: Users: elmir: scratch: nureth_papers_today~copy: 253_Final Paper. doc}$

Tests with heavy non condensable gases lead to the same kind of results. Examples of results are presented on Figure 8 and Figure 9 for Test 204b (with CO₂ injection) and on Figure 10 and Figure 11 for Test 205 (with helium injection). Numerical and experimental results are in good concordance: the pressure levels during the sump evaporation steady-state are well recovered by numerical calculations, for the ASTEC/CPA as well as for the TONUS code. In those figures, the transient phase of water injection is not perfectly simulated, so that the differences obtained during this phase are not relevant. An interesting result concerns the TOSQAN Test 205, in which helium is injected. It can be seen that a pressure increase (around 15'000 s until 20'000 s) is observed experimentally, which corresponds to an evaporative sump state without any wall condensation: the absence of wall condensation is due to the fact that helium is, at the beginning, mainly concentrated in the upper part of the vessel, above the injection pipe and facing the condensing wall region. A helium layer is thus modifying the gas mixture close to the condensing wall, and inhibits steam condensation. As a result, pressure is increasing inside the vessel. The helium in the vessel upper part is slowly mixed with the bottom part of the vessel, modifying the properties of the gas mixture close to the walls and allowing wall condensation to begin. As soon as condensation begins, the pressure decreases and a new steady-state is obtained. In the numerical calculations, this phenomenon is not recovered: in ASTEC/CPA, this cannot be recovered since the choice has been made to use a simple nodalization and not to divide into many zones the free volume of the TOSQAN vessel. Dividing in more zones this free volume would need the adaptation of different pressure loss coefficients, without enough argument to justify such adaptation, in this specific case. Concerning TONUS code, the specific pressure evolution attributed to wall condensation in the presence of a light gas is also not recovered. One explanation for that could be that the turbulence model (mixing length model) leads probably to a high gas mixing, avoiding helium enrichment in the condensing zone region. As a conclusion, the effect on pressure observed here is not well recovered by both codes, but this is rather attributed to a wrong modelling of the gaseous mixing in the presence of helium, than to the sump modelling. It confirms conclusions drawn in many past projects on the needs of better evaluation of the transient evolution of gas distribution, especially in the presence of light non condensable gases, which is an important topic for hydrogen risk evaluation.

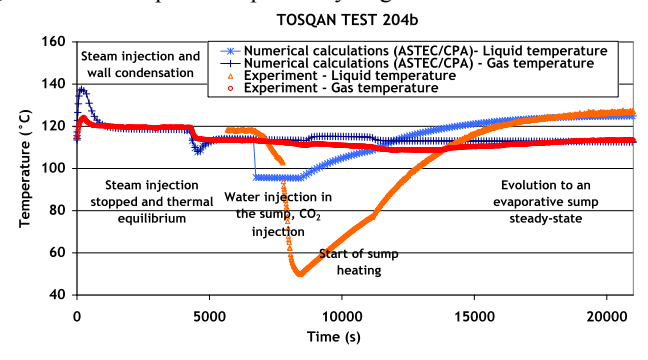


Figure 8: Mean gas temperature and mean liquid temperature time evolutions, TOSQAN Test 204b, ASTEC/CPA results compared to experiment.

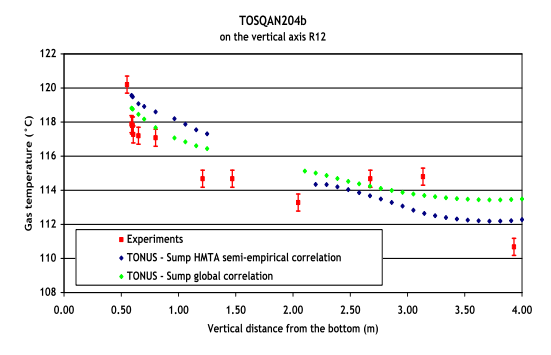


Figure 9: Local gas temperature vertical profile on TOSQAN axis during final equilibrium, TOSQAN Test 204b, TONUS-CFD results compared to experiment for both implemented sump models.

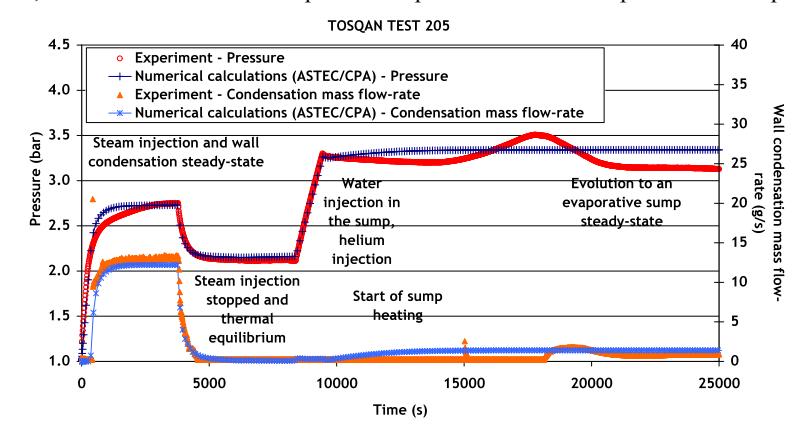


Figure 10: Pressure and condensation mass flow-rate time evolutions, TOSQAN Test 205, ASTEC/CPA results compared to experiment.

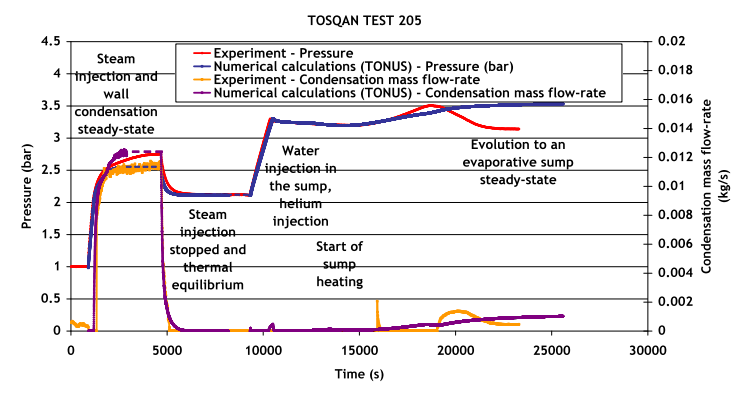


Figure 11: Pressure and condensation mass flow-rate time evolutions, TOSQAN Test 205, TONUS-CFD results compared to experiment

 $Macintosh\ HD: Users: elmir: scratch: nureth_papers_today\ copy: 253_Final Paper. document to the paper of the paper of$

Transient sump tests are calculated with ASTEC/CPA, for a low and a high depressurization rate (Figure 12 and Figure 13). The calculated pressure curves are in good agreement with the experiments. However, for the low depressurization rate test, no wall condensation is observed in the experiments, whereas the ASTEC/CPA calculations show a significant condensation rate. For the high depressurization rate test, calculations and experiments are in good agreement, both indicating no wall condensation. One explanation for these results could be that, in the case of low depressurization rate, the low nodalization of the ASTEC/CPA calculation does not allow to catch the phenomena that occure. These discrepancies would thus not be due to sump modelling, but would be rather due to different transient gaseous thermalhydraulics conditions in the containment atmosphere not considered in the calculations. However, this cannot be confirmed at this stage. This effect could be investigated with more sensitivity calculations in the future.

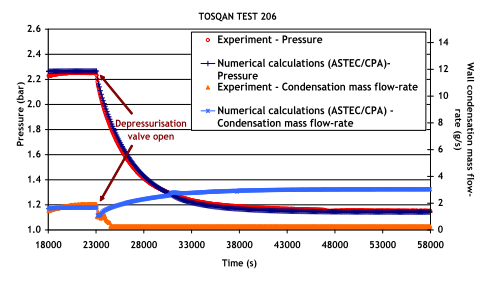


Figure 12: Pressure and condensation mass flow-rate time evolutions, TOSQAN Test 206, ASTEC/CPA results compared to experiment.

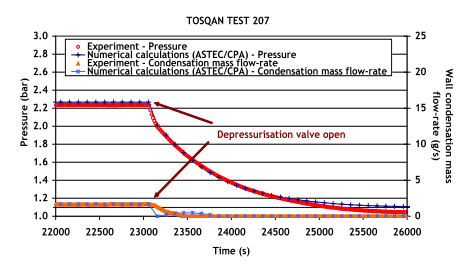


Figure 13: Pressure and condensation mass flow-rate time evolutions, TOSQAN Test 207, ASTEC/CPA results compared to experiment.

5. Conclusion

Numerical calculations of sump tests have been performed with a lumped-parameter code (ASTEC/CPA) and a CFD code (TONUS-CFD), for which two specific sump evaporation models have been added as user-defined functions. Results are compared with experiments on the TOSQAN facility where an evaporative sump is obtained under typical conditions of a severe accident in Nuclear Power Plants. Calculations of air-steam tests under steady-state evaporative sump conditions, as well as tests with heavy gas injections, show a good agreement with the experiments, indicating a good behaviour of the sump models in both codes. Calculations of air-steam-helium tests show some different behaviour in the vessel pressure evolution that is probably not due to the sump modelling but to the gas mixing modelling involved for the calculations. For ASTEC/CPA, it is known that a finer nodalization is requested for a better gas mixing evaluation. For TONUS-CFD, turbulence modelling under turbulent natural convection needs some improvement. Concerning depressurization tests, the pressure

evolution is well recovered in the ASTEC/CPA calculations, even if, for the slow depressurization test, calculations lead to significant wall condensation whereas in the experiment, no condensation occurs. As a main conclusion, it can be said that the validation of sump modelling in both codes is good and that the remaining discrepancies between codes and experiments are probably due to the gas distribution modelling, especially with light gas and under specific transient conditions. Knowing the importance of gas distribution for the evaluation of hydrogen risk in case of severe accident in nuclear power plant, code validations under transient conditions and with light gas are still needed.

6. References

- [1] S. Kudriakov, F. Dabbene, E. Studer, A. Beccantini, J.P. Magnaud, H. Paillère, A. Bentaib, A. Bleyer, J. Malet, E. Porcheron, C. Caroli "The TONUS CFD code for hydrogen risk analysis: Physical models, numerical schemes and validation matrix" *Nuclear Engineering and Design*, 2008, Vol. 238(3)
- [2] J. Bestele, W. Klein-Hessling "ASTEC V0, CPA Module, Containment Thermalhydraulics and Aerosol and Fission Product Behaviour, User Guidelines, rev 0" 2000, GRS Report ASTEC-VO/DOC/00-14
- [3] J. Malet, E. Porcheron, J. Vendel "OECD International Standard Problem ISP-47 on containment thermal-hydraulics Conclusions of the TOSQAN part" *Nuclear Engineering and Design*, 2010, Vol. 240, pp. 3209–3220
- [4] J. Malet, L. Blumenfeld, S. Arndt, M. Babic, A. Bentaib, F. Dabbene, P. Kostka, S. Mimouni, M. Movahed, S. Paci, Z. Parduba, J. Travis, E. Urbonavicius, "Sprays in Containment: Final results of the SARNET Spray Benchmark", accepted, to be published in *Nuclear Engineering and Design*, 2011
- [5] H. Karwat, "ISP-23, Rupture of large diameter pipe in the HDR containment" 1989, OECD/NEA/CSNI Report 160
- [6] H. Karwat, "ISP-29: Distribution of hydrogen within the HDR containment under severe accident conditions" 1993, OECD/NEA/CSNI Report R(93)4
- [7] M. Firnhaber, T.F. Kanzleiter, S. Schwarz, G. Weber, "ISP-37: VANAM M3 A Multi compartment aerosol depletion test with hygroscopic aerosol material" 1996, OCDE/NEA/CSNI Report R(96)26
- [8] O. Auban, J. Malet, P. Brun, J. Brinster, J.J. Quillico, E. Studer. "Implementation of gas concentration measurement systems using mass spectrometry in containment thermalhydraulics test facilities: different approaches for calibration and measurement with steam/air/helium mixtures", 2003, NURETH-10 conference, Seoul, Korea
- [9] E. Porcheron, L. Thause, J. Malet, P. Cornet, P. Brun, J. Vendel "Simultaneous application of spontaneous Raman scattering and LDV, PIV for steam/ airflow characterization" 2002, <u>10th</u> International Symposium on Flow Visualization, Kyoto, Japan
- [10] T. Gelain, J. Malet, E. Porcheron, P. Lemaitre, J. Vendel "Evaporation over the water sump surface in containment studies: presentation of the TOSQAN sump test matrix" 2009 NURETH-13 conference, Kanazawa City, Japan, September 27-October 2
- [11] E. Porcheron, P. Lemaitre, "TOSQAN sump tests" 2010, ICONE conference, China
- [12] J. Malet, M. Bessiron, C. Perrotin "Modelling of water sump evaporation in a CFD code for nuclear containment studies", accepted, to be published in *Nuclear Engineering and Design*, 2011
- [13] F. Dabbenne, "TONUS-0D 2005.1 physical models" 2005, Technical Report CEA DEN/SFME/LTMF/RT/05-038/A
- [14] L.M.K. Boelter, H.S. Gordon, J.R. Griffin "Free Evaporation into Air of Water from a Free Horizontal Quiet Surface" *Industrial and Engineering Chemistry*, 1946, Vol. 38, No. 6, pp596-600